ACS OMEGA

http://pubs.acs.org/journal/acsodf

Article

MOF-Derived Fe-Doped Ni@NC Hierarchical Hollow Microspheres as an Efficient Electrocatalyst for Alkaline Oxygen Evolution Reaction

Qianqian Wang, Yanyan Song,* Deshuai Sun,* and Lixue Zhang*

Cite This: *ACS Omega* 2021, 6, 11077−11082

Read Online

ACCESS | Metrics & More | Article Recommendations

ABSTRACT: The development of low-cost and efficient electrocatalysts for oxygen evolution reaction (OER) is of great importance for producing hydrogen via water splitting. Metal−organic frameworks (MOFs) provide an opportunity for the facile preparation of high-efficiency OER electrocatalysts. In this work, we prepared iron-doped nickel nanoparticles encapsulated in nitrogen-doped carbon microspheres (Fe-Ni@NC) with a unique hierarchical porous structure by directly pyrolyzing the MOF precursor for effectively boosting OER. The Fe doping has a significant enhancement effect on the catalytic performance. The optimized Fe (5%)-Ni@NC catalyst represents a remarkable activity with an overpotential of 257 mV at 10 mA cm^{-2} and superior stability toward OER in 1.0 M KOH.

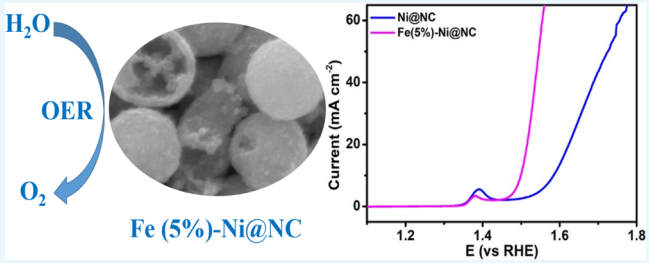

INTRODUCTION

The current energy crisis and environmental issues make it particularly important to explore sustainable energy to reduce the use of fossil energy. Electrochemical water splitting as a potential solution for green hydrogen production has been widely studied.[1] However, as a multistep proton-coupled electron transfer process, the kinetics of oxygen evolution reaction (OER) is very sluggish, which limits the practical use of electrochemical water splitting.[2] To expedite the OER process, electrocatalysts with high activity and good stability are needed. Hitherto, noble metal-based catalysts (RuO_2 or IrO_2) have been recognized as the most efficient catalysts toward OER, but their scarcity and high cost impede the wide-scale industrialization of OER technologies.[3−5] Thus, it is highly imperative to explore cost-effective and reserve-abundant alternative electrocatalysts for OER.

Presently, transition metals (such as Ni, Co, Fe, and Mn) are proverbially recognized as potential alternatives for their reasonable cost and natural abundance.[6−9] Among these systems, Ni-based catalysts have broadly attracted attention and shown promising activities.[10,11] Reasonable composition control and structure design can further enhance the OER performance of Ni-based catalysts. For example, recent studies have proved that Fe doping into Ni-based catalysts can efficiently adjust the electronic structure, improve the electrical conductivity, and expose more surface area.[12,13] Taken together, Fe-doped Ni-based catalysts are reasonably expected to provide more favorable OER performance. However, the preparation of Fe-doped Ni-based OER electrocatalysts is quite challenging, and a facile synthetic strategy is highly desired.

Metal−organic frameworks (MOFs) have been widely used in adsorption, energy storage, drug delivery, catalysis, sensors, and other fields due to their highly adjustable characteristics in terms of the composition, structure, and pore size. The characteristics of MOFs also endow them as very promising precursors for the preparation of high-efficiency electrocatalysts.[14−17] Herein, we report the synthesis of Fe-doped Ni nanoparticles encapsulated in nitrogen-doped carbon (Fe-Ni@NC) hierarchical porous microspheres by directly pyrolyzing the MOF precursor. The microspherical Ni-based MOFs containing minor amounts of Fe were first synthesized by solvothermal reaction,[18,19] which were then converted into Fe-Ni@NC hierarchical porous microspheres by a simple calcination process. Benefiting from the Fe doping and hierarchical porous structure, the prepared Fe-doped Ni@NC electrocatalyst presents remarkable oxygen evolution catalytic performance in 1.0 M KOH. We also compared the influence of the Fe doping level on their catalytic properties, and the optimized Fe(5%)-Ni@NC catalyst can realize an overpotential of 257 mV at 10 mA cm^{-2} toward OER.

Received: March 2, 2021
Accepted: April 1, 2021
Published: April 13, 2021

https://doi.org/10.1021/acsomega.1c01132
ACS Omega 2021, 6, 11077−11082

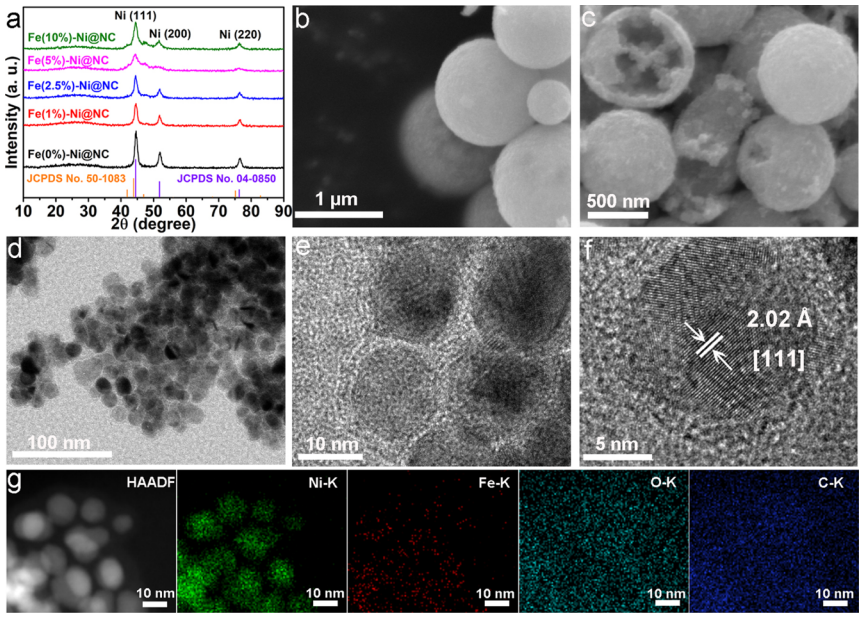

Figure 1. (a) XRD patterns of both Ni@NC and Fe-doped Ni@NC samples. (b) SEM image of Fe(5%)-Ni MOF. (c) SEM, (d–f) TEM, and HRTEM images of the Fe(5%)-Ni@NC sample. (g) Elemental mapping images of the Fe(5%)-Ni@NC sample.

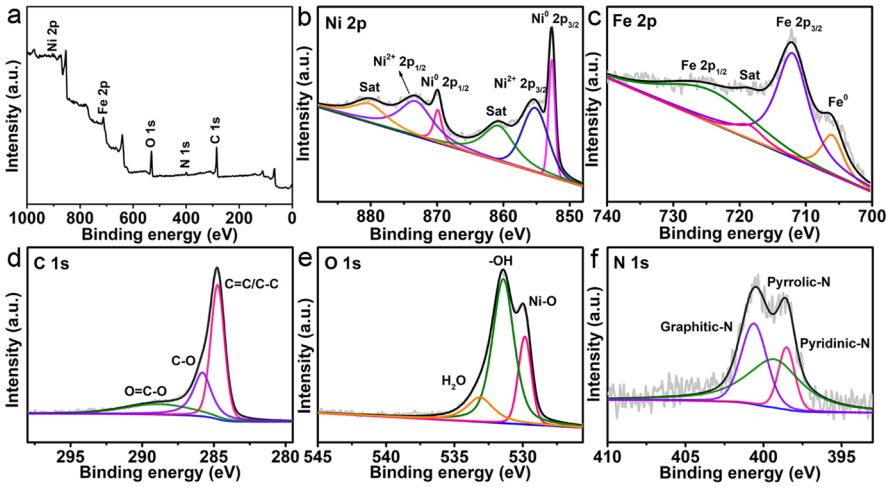

Figure 2. (a) XPS survey spectra of Fe(5%)-Ni@NC. The high-resolution XPS spectra of Fe(5%)-Ni@NC in (b) Ni 2p, (c) Fe 2p, (d) C 1s, (e) O 1s, and (f) N 1s regions.

RESULTS AND DISCUSSION

X-ray diffraction (XRD) measurements were conducted to validate the composition and the crystal structure of the obtained MOF-derived samples. The XRD patterns of Fe(5%)-Ni@NC show three characteristic diffraction peaks at 44.3, 51.6, and 76.2°, which can correspond well to (111), (200), and (220) crystal planes of metallic Ni, respectively, (JCPDS no. 04-0850) (Figure 1a). It is worth mentioning that no additional diffraction peaks of Fe phases can be observed due to the similar atomic size as Ni.[20] Subsequently, the morphologies and microstructures of the prepared MOF and MOF-derived samples were observed by scanning electron microscopy (SEM) and transmission electron microscopy (TEM) experiments. Figure 1b shows that the prepared Fe(5%)-Ni MOF samples are micrometer spheres with a rough surface. The microspherical structure is believed to be formed via an Ostwald ripening process, in which PVP also plays a very critical role.[18,19] After the pyrolysis in Ar, the Fe(5%)-Ni MOF was converted into Fe-doped Ni nanoparticles encapsulated in nitrogen-doped carbon, and the obtained Fe(5%)-Ni@NC could perfectly maintain the spherical structure of the Fe(5%)-Ni MOF without obvious agglomeration or structural collapse (Figure 1c).[21] In addition, Fe(5%)-Ni@NC has a much rougher surface compared with the Fe(5%)-Ni MOF. TEM images (Figure 1d,e) show that Fe(5%)-Ni@NC is composed of many nanoparticles around with carbon layers. HRTEM (Figure 1f) displays the interplanar of the lattice fringes as 0.202 nm, corresponding to the (111) crystal plane of Ni. Elemental mapping images in Figure 1g reveal the successful doping of Fe and the uniform distribution of Ni, Fe, O, and C in the prepared Fe(5%)-Ni@NC sample. The O element may come from the adsorbed oxygen and a small amount of metal oxides in the sample.[22]

X-ray photoelectron spectroscopy (XPS) was used to characterize the chemical states of elements in the Fe (5%)-Ni@NC sample. The survey spectra indicate the co-existence

https://doi.org/10.1021/acsomega.1c01132
ACS Omega 2021, 6, 11077−11082

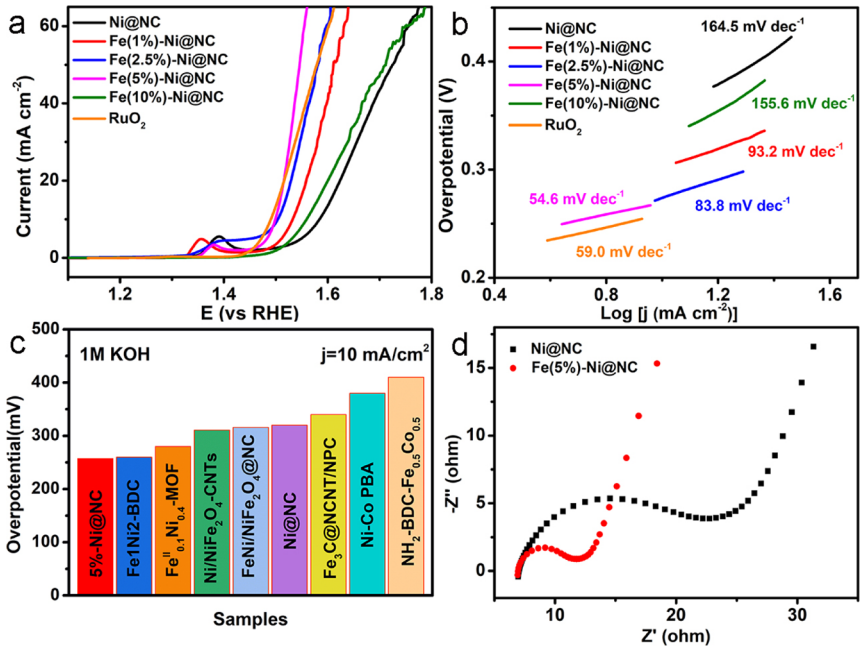

Figure 3. (a) LSV curves of Ni@NC, Fe(1%)-Ni@NC, Fe(2.5%)-Ni@NC, Fe(5%)-Ni@NC, Fe(10%)-Ni@NC, and RuO_2 in 1.0 M KOH at 5 mV s^{-1}. (b) Tafel plots of different catalysts. (c) Comparison of the overpotential at 10 mA·cm^{-2} between Fe(5%)-Ni@NC and some recently reported similar electrocatalysts. (d) Nyquist plots for Ni@NC and Fe(5%)-Ni@NC.

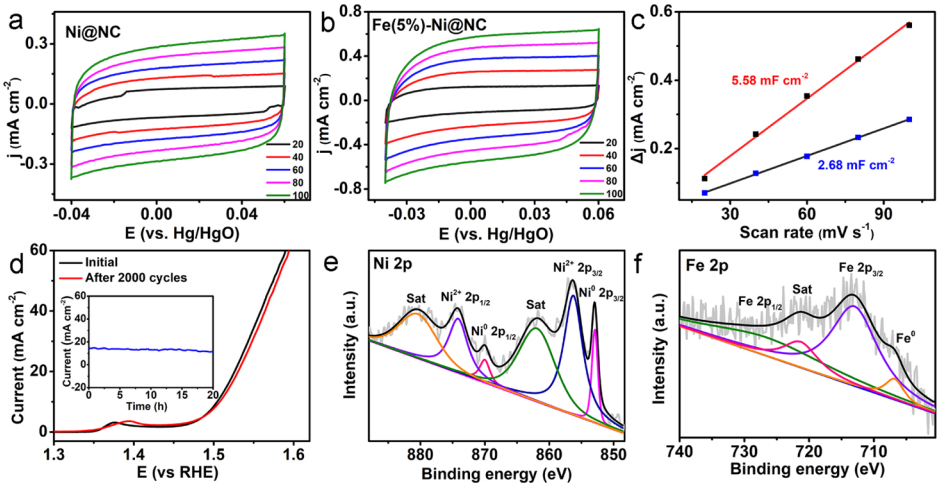

Figure 4. CVs of (a) Ni@NC and (b) Fe(5%)-Ni@NC at scan rates of 20, 40, 60, 80, and 100 mV s^{-1} in 1.0 M KOH. (c) Corresponding capacitive currents at 0.01 V versus Hg/HgO as a function of scan rates for Ni@NC and Fe(5%)-Ni@NC. (d) Polarization curves of Fe(5%)-Ni@NC before and after 2000 cycles in 1.0 M KOH, and the inset is a chronoamperometric curve of Fe(5%)-Ni@NC at 1.50 V (vs RHE) for 20 h. XPS spectra of Fe(5%)-Ni@C after stability test in (e) Ni 2p and (f) Fe 2p regions.

of Fe, Ni, C, N, and O (Figure 2a). In the high-resolution Ni 2p spectra of Fe(5%)-Ni@NC (Figure 2b), the dominant peaks centered at 852.7 and 869.9 eV confirm the formation of metallic Ni,[23] and the peaks located at 855.2 and 873.2 eV are ascribed to Ni^{2+}, which is an indicator of surface oxidation of metallic Ni. In Figure 2c, the peak at 706.1 eV suggests the existence of metallic Fe. The Fe 2p spectra also show Fe $2p_{3/2}$ and Fe $2p_{1/2}$ for Fe^{2+} at 712.0 and 724.4 eV, respectively.[24] In the C 1s region (Figure 2d), the peaks of 284.7, 285.8, and 288.8 eV correspond to the C═C/C−C, C−O, and O−C═O, respectively. The peaks at 531.4 and 533.1 eV in the O 1s spectra should be ascribed to the surface-adsorbed hydroxyl groups and adsorbed water, respectively, and the peak at 529.8 eV should be attributed to lattice oxygen of minor metal oxides in the sample (Figure 2e).[25] The three peaks located at 398.5, 399.3, and 400.6 eV in N 1s spectra should be assigned to pyridine N, pyrrole N, and graphite N, respectively (Figure 2f). This result implies that the N element has been successfully incorporated into carbon.[26] The abovementioned results indicate that Fe-doped Ni@NC hierarchical hollow microspheres have been successfully synthesized via the MOF conversion strategy.

Linear sweeping voltammetry (LSV) tests were performed in 1.0 M KOH to evaluate the electrocatalytic OER performance of Fe-doped Ni@NC using a three-electrode system. For comparison, under the same conditions, Ni@NC, Fe(1%)-Ni@NC, Fe(2.5%)-Ni@NC, Fe(10%)-Ni@NC, and RuO_2 were also tested (Figure 3a). All the MOF-derived Ni-based

https://doi.org/10.1021/acsomega.1c01132
ACS Omega 2021, 6, 11077−11082

catalysts show good OER catalytic performances, in which the hierarchical hollow microstructure should contribute much in affording numerous active sites and achieving fast mass transfer.[18,19] More importantly, the Fe-doped Ni@NC samples exhibit even lower overpotentials and smaller Tafel slopes than the pure Ni@NC sample (Figure 3a,b), indicating that the Fe dopant further enhances the electrocatalytic activity of Ni@NC. Fe doping can efficiently modulate the electronic structure of materials, thus improving the intrinsic catalytic activity of Ni-based catalysts.[12,13] We should emphasize that Fe(5%)-Ni@NC exhibits the smallest overpotential of 257 mV at 10 mA cm^{-2} among the prepared Ni@NC catalysts, even outperforming the RuO_2 catalyst at high current density. The Tafel slope of Fe(5%)-Ni@NC is identified to be 54.6 mV dec^{-1}, which is smaller than that of other Ni@NC catalysts (Figure 3b). It reveals the very fast OER kinetics on Fe (5%)-Ni@NC. Compared with the recently reported similar electrocatalysts (Figure 3c), Fe(5%)-Ni@NC also exhibits comparable and even better OER performance under alkaline conditions.[27−34] In addition, the electrochemical impedance spectroscopy (EIS) data (Figure 3d) show that Fe(5%)-Ni@NC possesses a smaller radius of the semicircle than Ni@NC, implying that Fe(5%)-Ni@NC has a lower charge transfer resistance and thus faster OER kinetics.[35]

Furthermore, the double-layer capacitances (C_{dl}) were measured in the non-faradaic voltage range to estimate the ECSA of the Fe(5%)-Ni@NC and Ni@NC samples (Figure 4a−c). The C_{dl} of Fe (5%)-Ni@NC is 5.58 mF cm^{-2}; meanwhile, the C_{dl} of Ni@NC is only 2.68 mF cm^{-2}. Therefore, the ECSA of Fe(5%)-Ni@NC is higher than that of Ni@NC, resulting in the more catalytic active sites for Fe(5%)-Ni@NC. These results indicate that Fe doping into Ni@NC is also beneficial to boost the electrocatalytic activity via improving the charge transfer and providing more active sites.

The electrochemical stability is another important indicator to evaluate the performance of the electrocatalyst.[36] As shown in Figure 4d, after 2000 consecutive cyclic voltammetry (CV) scanning cycles at 100 mV s^{-1} between 1.3 and 1.8 V [vs reversible hydrogen electrode (RHE)], the OER electrocatalytic performance of Fe(5%)-Ni@NC shows no apparent change. Moreover, the chronoamperometric measurement for Fe(5%)-Ni@NC was performed constantly at 1.50 V (vs RHE). The inset of Figure 4d shows that Fe(5%)-Ni@NC maintains its current density for least 20 h without clear deterioration, implying that Fe(5%)-Ni@NC has excellent catalytic durability. The XPS spectrum in the Ni 2p region of the catalyst after the stability test showed that the peaks at 855.2 and 873.2 eV increased significantly (Figure 4e), which should be caused by the formation of NiOOH active sites during the electrolysis process. In the Fe 2p region (Figure 4f), the characteristic peaks of 706.6 eV are obviously reduced, and it should be due to the formation of high-valence Fe, which in turn leads to the electronic structure optimization of Ni and the enhancement of OER activity.[37]

CONCLUSIONS

In summary, we report a simple synthesis of MOF-derived Fe-doped Ni@NC with a hierarchical hollow structure. Due to the positive effects of Fe doping and the hierarchical porous structure, the prepared Fe(5%)-Ni@NC catalyst represents remarkable activity and durability toward OER in 1.0 M KOH. It can reach 10 mA cm^{-2} only by delivering an overpotential of 257 mV, and the Tafel slope is only 54.6 mV dec^{-1}. Such a performance is very comparable with that of the commercial RuO_2 catalyst. The facile and low-cost preparation, along with the high OER electrocatalytic activity and long-term stability, makes the prepared Fe-doped Ni@NC catalyst hold a potential application in electrochemical water splitting.

EXPERIMENTAL SECTION

Preparation of Ni@NC. Ni MOFs were synthesized by a hydrothermal method.[17,18] Typically, 3 mmol $NiCl_2{\cdot}6H_2O$, 1.5 mmol Trimesic acid, and 3 g of PVP were dispersed into 60 mL of the mixed solution (ethanol: DMF: ultrapure water = 1:1:1) with stirring for 30 min. The clarified solution was transferred to a 100 mL Teflon-lined stainless-steel autoclave. It was heated at 150 °C for 9 h. Subsequently, the products were centrifuged and washed with ethanol several times and dried at 60 °C for 12 h to obtain the Ni MOF precursor. Finally, to prepare Ni@NC, Ni MOFs were annealed at 450 °C in an argon atmosphere for 2 h.

Preparation of Fe-Doped Ni@NC. In the synthesis of Fe(X %)-doped Ni MOFs, different molar contents (X = 1/2.5/5/10 % × 3.0 mmol) of $FeCl_3{\cdot}6H_2O$ were added to 3.0 × (1 − X) mmol $NiCl_2{\cdot}6H_2O$, 1.5 mmol trimesic acid, and 3.0 g of PVP. The other steps are the same as in the synthesis of Ni@NC. Finally, the Fe (1/2.5/5/10%)-Ni@NC was obtained.

Material Characterization. XRD patterns were detected on a DX2700 equipment (Dandong, China). SEM experiments were performed on a JSM-7001F (JEOL, Tokyo, Japan) microscope. TEM images were acquired on a JEM-2100F microscope with an accelerating voltage of 200 kV (JEOL, Tokyo, Japan). XPS was performed on an ESCALABMK II spectrometer. The analyses of XPS data were completed with XPSPEAK. The charge correction was performed using the binding energy of C 1s (284.8 eV) as the reference. Before fitting, a proper baseline was added to the spectra. The following protocols were obeyed during peak fitting. According to the standard library, the distances were fixed for two peaks of the same chemical state and the half peak width was kept consistent. All peak positions were determined from the literature. Finally, each area was carefully adjusted to make the fitted data close to raw data.

Electrochemical Measurements. The electrochemical testing instrument is an electrochemical workstation (VSP-300, BioLogic, France). It adopts a three-electrode system: the catalyst-loaded glassy carbon electrode (0.07065 cm^{-2}), platinum wire, and Hg/HgO electrode are the working electrode, counter electrode, and reference electrode, respectively. iR correction was applied to all the LSV curves, and all potentials were converted into the RHE.

$$E_{RHE} = E_{Hg/HgO} + 0.098\ V + 0.0592pH$$

Preparation of the catalyst ink: 5 mg of the catalyst was spread in a 1 mL solution (the volume ratio of ethanol and water is 1:1) containing 20 μL of Nafion, which was then sonicated for several hours to obtain a uniformly dispersed catalyst ink. The working electrode was prepared by dropping 5 μL of ink on the glassy carbon electrode. EIS test was performed at open-circuit voltage with an amplitude of 5 mV and frequencies ranging from 10^6 to 0.01 Hz.

https://doi.org/10.1021/acsomega.1c01132
ACS Omega 2021, 6, 11077−11082

AUTHOR INFORMATION

Corresponding Authors

Yanyan Song − *College of Chemistry and Chemical Engineering, State Key Laboratory of Bio-fibers and Eco-textiles, Qingdao University, Qingdao 266071, Shandong, P. R. China*; Email: songyanyan1103@163.com

Deshuai Sun − *College of Chemistry and Chemical Engineering, State Key Laboratory of Bio-fibers and Eco-textiles, Qingdao University, Qingdao 266071, Shandong, P. R. China*; orcid.org/0000-0002-4187-8886; Email: luckysds@qdu.edu.cn

Lixue Zhang − *College of Chemistry and Chemical Engineering, State Key Laboratory of Bio-fibers and Eco-textiles, Qingdao University, Qingdao 266071, Shandong, P. R. China*; orcid.org/0000-0003-3430-4988; Email: zhanglx@qdu.edu.cn

Author

Qianqian Wang − *College of Chemistry and Chemical Engineering, State Key Laboratory of Bio-fibers and Eco-textiles, Qingdao University, Qingdao 266071, Shandong, P. R. China*

Complete contact information is available at: https://pubs.acs.org/10.1021/acsomega.1c01132

Author Contributions

All authors have given approval to the final version of the manuscript.

Notes

The authors declare no competing financial interest.

ACKNOWLEDGMENTS

This work was supported by the National Natural Science Foundation of China (nos. 22075159 and 21775078) and Youth Innovation Team Project of Shandong Provincial Education Department (no. 2019KJC023).

REFERENCES

(1) Song, J.; Wei, C.; Huang, Z.-F.; Liu, C.; Zeng, L.; Wang, X.; Xu, Z. J. A Review on Fundamentals for Designing Oxygen Evolution Electrocatalysts. *Chem. Soc. Rev.* **2020**, *49*, 2196−2214.

(2) Suen, N.-T.; Hung, S.-F.; Quan, Q.; Zhang, N.; Xu, Y.-J.; Chen, H. M. Electrocatalysis for the Oxygen Evolution Reaction: Recent Development and Future Perspectives. *Chem. Soc. Rev.* **2017**, *46*, 337−365.

(3) Wei, Z.-X.; Zhu, Y.-T.; Liu, J.-Y.; Zhang, Z.-C.; Hu, W.-P.; Xu, H.; Feng, Y.-Z.; Ma, J.-M. Recent Advance in Single-Atom Catalysis. *Rare Met.* **2021**, *40*, 767−789.

(4) Wang, C.; Lan, F.; He, Z.; Xie, X.; Zhao, Y.; Hou, H.; Guo, L.; Murugadoss, V.; Liu, H.; Shao, Q.; Gao, Q.; Ding, T.; Wei, R.; Guo, Z. Iridium-Based Catalysts for Solid Polymer Electrolyte Electrocatalytic Water Splitting. *ChemSusChem* **2019**, *12*, 1576−1590.

(5) Yu, J.; He, Q.; Yang, G.; Zhou, W.; Shao, Z.; Ni, M. Recent Advances and Prospective in Ruthenium-Based Materials for Electrochemical Water Splitting. *ACS Catal.* **2019**, *9*, 9973−10011.

(6) Liu, J.; Ma, J.; Zhang, Z.; Qin, Y.; Wang, Y.-j.; Wang, Y.; Tan, R.; Duan, X.; Tian, T. Z.; Zhang, C. H.; Xie, W. W.; Li, N.-W.; Yu, L.; Yang, C.; Zhao, Y.; Zia, H.; Nosheen, F.; Zheng, G.; Gupta, S.; Wu, X.; Wang, Z.; Qiu, J.; Zhou, G.; Xu, L.; Liu, K.; Fu, J.; Liu, M.; Choi, S.-I.; Xie, J.; Peng, X.; Li, T.; Lin, G.; Wang, J.; Han, J.; Liang, H.; Li, S.; Zhang, X.; Zhu, Y.; He, T.; Cui, X.; Wang, H.; Wei, Z.; Liu, Q.; Fan, G.; Liu, Q.; Sun, X.; Feng, Y.; Liu, Y.; Chu, K.; Qiu, Y.; Liu, X. 2020 Roadmap on Electrocatalysts for Green catalytic processes. *JPhys Mater.* **2020**, DOI: 10.1088/2515-7639/abd596.

(7) Wang, H.; Zhu, S.; Deng, J.; Zhang, W.; Feng, Y.; Ma, J. Transition metal carbides in electrocatalytic oxygen evolution reaction. *Chin. Chem. Lett.* **2021**, *32*, 291−298.

(8) Yu, J.; Lv, C.; Zhao, L.; Zhang, L.; Wang, Z.; Liu, Q. Reverse Microemulsion-Assisted Synthesis of $NiCo_2S_4$ Nanoflakes Supported on Nickel Foam for Electrochemical Overall Water Splitting. *Adv. Mater. Interfaces* **2018**, *5*, 1701396.

(9) Jin, L.; Pang, H. CoP@SiO_2 Nanoreactors: A Core-Shell Structure for Efficient Electrocatalytic Oxygen Evolution Reaction. *Chin. Chem. Lett.* **2020**, *31*, 2300−2304.

(10) Wang, Z.; Zhang, L. Nickel Ditelluride Nanosheet Arrays: A Highly Efficient Electrocatalyst for the Oxygen Evolution Reaction. *ChemElectroChem* **2018**, *5*, 1153−1158.

(11) Sivanantham, A.; Ganesan, P.; Shanmugam, S. Hierarchical $NiCo_2S_4$ Nanowire Arrays Supported on Ni Foam: An Efficient and Durable Bifunctional Electrocatalyst for Oxygen and Hydrogen Evolution Reactions. *Adv. Funct. Mater.* **2016**, *26*, 4661−4672.

(12) Anantharaj, S.; Kundu, S.; Noda, S. "The Fe Effect": A Review Unveiling the Critical Roles of Fe in Enhancing OER Activity of Ni and Co Based Catalysts. *Nano Energy* **2021**, *80*, 105514.

(13) Zhu, W.; Zhu, G.; Hu, J.; Zhu, Y.; Chen, H.; Yao, C.; Pi, Z.; Zhu, S.; Li, E. Poorly Crystallized Nickel Hhydroxide Carbonate Loading with Fe^{3+} ions as Improved Electrocatalysts for Oxygen Evolution. *Inorg. Chem. Commun.* **2020**, *114*, 107851.

(14) Du, J.; Li, F.; Sun, L. Metal-Organic Frameworks and their Derivatives as Electrocatalysts for the Oxygen Evolution Reaction. *Chem. Soc. Rev.* **2021**, *50*, 2663.

(15) Yang, D.; Chen, Y.; Su, Z.; Zhang, X.; Zhang, W.; Srinivas, K. Organic Carboxylate-Based MOFs and Derivatives for Electrocatalytic Water Oxidation. *Coord. Chem. Rev.* **2021**, *428*, 213619.

(16) Li, X.; Fan, M.; Wei, D.; Li, M.; Wang, Y. Unveiling the Real Active Sites of Ni Based Metal Organic Framework Electrocatalysts for the Oxygen Evolution Reaction. *Electrochim. Acta* **2020**, *354*, 136682.

(17) Fang, B.; Feng, L. PtCo-NC Catalyst Derived from the Pyrolysis of Pt-Incorporated ZIF-67 for Alcohols Fuel Electrooxidation. *Acta Phys.-Chim. Sin.* **2020**, *36*, 1905023.

(18) Wang, X.; Wu, X.-L.; Guo, Y.-G.; Zhong, Y.; Cao, X.; Ma, Y.; Yao, J. Synthesis and Lithium Storage Properties of Co_3O_4 Nanosheet-Assembled Multishelled Hollow Spheres. *Adv. Funct. Mater.* **2010**, *20*, 1680−1686.

(19) Zou, F.; Chen, Y.-M.; Liu, K.; Yu, Z.; Liang, W.; Bhaway, S. M.; Gao, M.; Zhu, Y. Metal Organic Frameworks Derived Hierarchical Hollow NiO/Ni/Graphene Composites for Lithium and Sodium Storage. *ACS Nano* **2016**, *10*, 377−386.

(20) Wang, P.; Pu, Z.; Li, Y.; Wu, L.; Tu, Z.; Jiang, M.; Kou, Z.; Amiinu, I. S.; Mu, S. Iron-Doped Nickel Phosphide Nanosheet Arrays: An Efficient Bifunctional Electrocatalyst for Water Splitting. *ACS Appl. Mater. Interfaces* **2017**, *9*, 26001−26007.

(21) Wang, L.; Geng, J.; Wang, W.; Yuan, C.; Kuai, L.; Geng, B. Facile Synthesis of Fe/Ni Bimetallic Oxide Solid-Solution Nanoparticles with Superior Electrocatalytic Activity for Oxygen Evolution Reaction. *Nano Res.* **2015**, *8*, 3815−3822.

(22) Liu, X.; Xu, D.; Wang, Q.; Zhang, L. Fabrication of 3D Hierarchical Byttneria Aspera-Like Ni@Graphitic Carbon Yolk-Shell Microspheres as Bifunctional Catalysts for Ultraefficient Oxidation/Reduction of Organic Contaminants. *Small* **2018**, *14*, No. e1803188.

(23) Li, T.; Luo, G.; Liu, K.; Li, X.; Sun, D.; Xu, L.; Li, Y.; Tang, Y. Encapsulation of Ni_3Fe Nanoparticles in N-Doped Carbon Nanotube-Grafted Carbon Nanofibers as High-Efficiency Hydrogen Evolution Electrocatalysts. *Adv. Funct. Mater.* **2018**, *28*, 1805828.

(24) Zhao, S.; Li, M.; Han, M.; Xu, D.; Yang, J.; Lin, Y.; Shi, N.-E.; Lu, Y.; Yang, R.; Liu, B.; Dai, Z.; Bao, J. Defect-Rich Ni_3FeN Nanocrystals Anchored on N-Doped Graphene for Enhanced Electrocatalytic Oxygen Evolution. *Adv. Funct. Mater.* **2018**, *28*, 1706018.

(25) Zhang, K.; Xia, X.; Deng, S.; Zhong, Y.; Xie, D.; Pan, G.; Wu, J.; Liu, Q.; Wang, X.; Tu, J. Nitrogen-Doped Sponge Ni Fibers as Highly

Efficient Electrocatalysts for Oxygen Evolution Reaction. *Nano−Micro Lett.* **2019**, *11*, 21.
(26) Xu, Y.; Tu, W.; Zhang, B.; Yin, S.; Huang, Y.; Kraft, M.; Xu, R. Nickel Nanoparticles Encapsulated in Few-Layer Nitrogen-Doped Graphene Derived from Metal-Organic Frameworks as Efficient Bifunctional Electrocatalysts for Overall Water Splitting. *Adv. Mater.* **2017**, *29*, 1605957.
(27) Hai, G.; Jia, X.; Zhang, K.; Liu, X.; Wu, Z.; Wang, G. High-Performance Oxygen Evolution Catalyst using Two-Dimensional Ultrathin Metal-Organic Frameworks Nanosheets. *Nano Energy* **2018**, *44*, 345−352.
(28) Zheng, F.; Xiang, D.; Li, P.; Zhang, Z.; Du, C.; Zhuang, Z.; Li, X.; Chen, W. Highly Conductive Bimetallic Ni−Fe Metal Organic Framework as a Novel Electrocatalyst for Water Oxidation. *ACS Sustainable Chem. Eng.* **2019**, *7*, 9743−9749.
(29) Zhang, D.; Huang, R.; Xie, H.; Li, R.; Liu, X.; Pan, M.; Lei, Y. Effect of the Valence State of Initial Iron Source on Oxygen Evolution Activity of Fe-Doped Ni-MOF. *Chem. Pap.* **2020**, *74*, 2775−2784.
(30) Ma, Y.; Dai, X.; Liu, M.; Yong, J.; Qiao, H.; Jin, A.; Li, Z.; Huang, X.; Wang, H.; Zhang, X. Strongly Coupled FeNi Alloys/$NiFe_2O_4$@Carbonitride Layers-Assembled Microboxes for Enhanced Oxygen Evolution Reaction. *ACS Appl. Mater. Interfaces* **2016**, *8*, 34396−34404.
(31) Yu, X.; Chen, G.; Wang, Y.; Liu, J.; Pei, K.; Zhao, Y.; You, W.; Wang, L.; Zhang, J.; Xing, L.; Ding, J.; Ding, G.; Wang, M.; Che, R. Hierarchical Coupling effect in Hollow Ni/$NiFe_2O_4$-CNTs Microsphere via Spray-Drying for Enhanced Oxygen Evolution Electrocatalysis. *Nano Res.* **2020**, *13*, 437−446.
(32) Zhao, P.; Hua, X.; Xu, W.; Luo, W.; Chen, S.; Cheng, G. Metal−Organic Framework-Derived Hybrid of Fe_3C Nanorod-Encapsulated, N-Doped CNTs on Porous Carbon Sheets for Highly Efficient Oxygen Reduction and Water Oxidation. *Catal. Sci. Technol.* **2016**, *6*, 6365−6371.
(33) Han, L.; Yu, X.-Y.; Lou, X. W. D. Formation of Prussian-Blue-Analog Nanocages via a Direct Etching Method and their Conversion into Ni-Co-Mixed Oxide for Enhanced Oxygen Evolution. *Adv. Mater.* **2016**, *28*, 4601−4605.
(34) Iqbal, B.; Saleem, M.; Arshad, S. N.; Rashid, J.; Hussain, N.; Zaheer, M. One-Pot Synthesis of Heterobimetallic Metal-Organic Frameworks (MOFs) for Multifunctional Catalysis. *Chem.—Eur. J.* **2019**, *25*, 10490−10498.
(35) Dong, C.; Kou, T.; Gao, H.; Peng, Z.; Zhang, Z. Eutectic-Derived Mesoporous Ni-Fe-O Nanowire Network Catalyzing Oxygen Evolution and Overall Water Splitting. *Adv. Energy Mater.* **2018**, *8*, 1701347.
(36) Zheng, F.; Zhang, Z.; Xiang, D.; Li, P.; Du, C.; Zhuang, Z.; Li, X.; Chen, W. Fe/Ni Bimetal Organic Framework as Efficient Oxygen Evolution Catalyst with Low Overpotential. *J. Colloid Interface Sci.* **2019**, *555*, 541−547.
(37) Li, N.; Bediako, D. K.; Hadt, R. G.; Hayes, D.; Kempa, T. J.; von Cube, F.; Bell, D. C.; Chen, L. X.; Nocera, D. G. Influence of Iron Doping on Tetravalent Nickel Content in Catalytic Oxygen Evolving Films. *Proc. Natl. Acad. Sci. U.S.A.* **2017**, *114*, 1486−1491.

https://doi.org/10.1021/acsomega.1c01132
ACS Omega 2021, 6, 11077−11082